Fraction estimation of small, dense LDL using autocorrelation function of dynamic light scattering

Suchin Trirongjitmoah[1]*, Toshihiro Sakurai[2], Kazuya Iinaga[3], Hitoshi Chiba[2] and Koichi Shimizu[1]

[1]*Graduate School of Information Science and Technology, Hokkaido University, W9, N14, Kita-ku, Sapporo 060-0814, Japan*

[2] *Faculty of Health Sciences, Hokkaido University, W5, N12, Kita-ku, Sapporo 060-0812, Japan*

[3] *Technical Service Section, Denka Seiken Co., Ltd., 3-4-2, Nihonbashi, Kayabacho, Chuo-ku, Tokyo 103-0025, Japan*

**suchin@bme.ist.hokudai.ac.jp*

Abstract: Small, dense low-density lipoprotein (sdLDL) in total LDL is strongly related with the cardiovascular risk level. An optical technique using dynamic light scattering (DLS) measurement is useful for point-of-care testing of sdLDL. However, the sdLDL fraction estimated from the particle size distribution in DLS data is sensitive to noise and artifacts. Therefore, we derived analytical solutions in a closed form to estimate the fraction of scatterers using the autocorrelation function of scattered light from a polydisperse solution. The effect of the undesired large particles can be eliminated by the pre-processing of the autocorrelation function. The proposed technique was verified using latex standard particles and LDL solutions. Results suggest the feasibility of this technique to estimate the sdLDL fraction using optical scattering measurements.

OCIS codes: (290.5850) Scattering, particles; (170.1470) Blood or tissue constituent monitoring.

References and links

1. Y. Hirowatari, H. Yoshida, H. Kurosawa, K. I. Doumitu, and N. Tada, "Measurement of cholesterol of major serum lipoprotein classes by anion-exchange HPLC with perchlorate ion-containing eluent," J. Lipid Res. **44**(7), 1404–1412 (2003).
2. S. Akita, F. M. Sacks, L. P. Svetkey, P. R. Conlin, G. Kimura; DASH-Sodium Trial Collaborative Research Group, "Effects of the Dietary Approaches to Stop Hypertension (DASH) diet on the pressure-natriuresis relationship," Hypertension **42**(1), 8–13 (2003).
3. F. M. Sacks, and H. Campos, "Clinical review 163: Cardiovascular endocrinology: Low-density lipoprotein size and cardiovascular disease: a reappraisal," J. Clin. Endocrinol. Metab. **88**(10), 4525–4532 (2003).
4. J. B. German, J. T. Smilowitz, and A. M. Zivkovic, "Lipoproteins: When size really matters," Curr. Opin. Colloid Interface Sci. **11**(2–3), 171–183 (2006).
5. W. Ensign, N. Hill, and C. B. Heward, "Disparate LDL phenotypic classification among 4 different methods assessing LDL particle characteristics," Clin. Chem. **52**(9), 1722–1727 (2006).
6. M. Rizzo, and K. Berneis, "Low-density lipoprotein size and cardiovascular risk assessment," QJM **99**(1), 1–14 (2005).
7. H. Wang, H. M. Wang, Q. H. Jin, H. Cong, G. S. Zhuang, J. L. Zhao, C. L. Sun, H. W. Song, and W. Wang, "Microchip-based small, dense low-density lipoproteins assay for coronary heart disease risk assessment," Electrophoresis **29**(9), 1932–1941 (2008).
8. H. Campos, E. Blijlevens, J. R. McNamara, J. M. Ordovas, B. M. Posner, P. W. Wilson, W. P. Castelli, and E. J. Schaefer, "LDL particle size distribution. Results from the Framingham Offspring Study," Arterioscler. Thromb. **12**(12), 1410–1419 (1992).
9. T. Hirano, Y. Ito, H. Saegusa, and G. Yoshino, "A novel and simple method for quantification of small, dense LDL," J. Lipid Res. **44**(11), 2193–2201 (2003).
10. F. Gonzalez, J. M. Saiz, F. Moreno, and P. J. Valle, "Application of a Laplace Transform Method to Binary-Mixtures of Spherical-Particles in Solution for Low Scattered Intensity," J. Phys. D Appl. Phys. **25**(3), 357–361 (1992).

#120694 - $15.00 USD Received 30 Nov 2009; revised 12 Feb 2010; accepted 22 Feb 2010; published 12 Mar 2010

11. J. R. Vega, L. M. Gugliotta, V. D. G. Gonzalez, and G. R. Meira, "Latex particle size distribution by dynamic light scattering: novel data processing for multiangle measurements," J. Colloid Interface Sci. **261**(1), 74–81 (2003).
12. C. B. Frantzen, L. Ingebrigtsen, M. Skar, and M. Brandl, "Assessing the accuracy of routine photon correlation spectroscopy analysis of heterogeneous size distributions," AAPS PharmSciTech **4**(3), 62 (2003).
13. M. Shibayama, T. Karino, and S. Okabe, "Distribution analyses of multi-modal dynamic light scattering data," Polymer (Guildf.) **47**(18), 6446–6456 (2006).
14. M. Schneider, and T. F. McKenna, "Comparative study of methods for the measurement of particle size and size distribution of polymeric emulsions," Part. Part. Syst. Char. **19**(1), 28–37 (2002).
15. H. Ruf, and B. J. Gould, "Size distributions of chylomicrons from human lymph from dynamic light scattering measurements," Eur. Biophys. J. Biophy. **28**(1), 1–11 (1998).
16. M. P. Cagigal, M. A. Rebolledo, and F. Moreno, "Determination of the radii and the concentration ratio in binary mixtures of spherical macromolecules from the measurement of $n^{(2)}(T)$," Appl. Opt. **23**(13), 2091–2096 (1984).
17. M. G. Rasteiro, C. C. Lemos, and A. Vasquez, "Nanoparticle characterization by PCS: The analysis of bimodal distributions," Particul. Sci. Technol. **26**(5), 413–437 (2008).
18. B. J. Berne, and R. Pecora, *Dynamic light scattering: with applications to chemistry, biology, and physics,* Dover ed. (Dover Publications, Mineola, N.Y., 2000).
19. A. Flamberg, and R. Pecora, "Dynamic Light-Scattering Study of Micelles in a High Ionic-Strength Solution," J. Phys. Chem. **88**(14), 3026–3033 (1984).
20. A. Lomakin, G. B. Benedek, and D. B. Teplow, "Monitoring protein assembly using quasielastic light scattering spectroscopy," Methods Enzymol. **309**, 429–459 (1999).
21. R. S. Stock, and W. H. Ray, "Interpretation of photon correlation spectroscopy data: A comparison of analysis methods," J. Polym. Sci., Polym. Phys. Ed. **23**(7), 1393–1447 (1985).
22. P. A. Hassan, and S. K. Kulshreshtha, "Modification to the cumulant analysis of polydispersity in quasielastic light scattering data," J. Colloid Interface Sci. **300**(2), 744–748 (2006).
23. A. Milat, *MATLAB: an introduction with applications,* 3rd ed. (Wiley Publications, N.Y., 2008).
24. D. O'Neal, P. Harrip, G. Dragicevic, D. Rae, and J. D. Best, "A comparison of LDL size determination using gradient gel electrophoresis and light-scattering methods," J. Lipid Res. **39**(10), 2086–2090 (1998).
25. J. A. Chouinard, A. Khalil, and P. Vermette, "Method of imaging low density lipoproteins by atomic force microscopy," Microsc. Res. Tech. **70**(10), 904–907 (2007).
26. V. M. Gun'ko, A. V. Klyueva, Y. N. Levchuk, and R. Leboda, "Photon correlation spectroscopy investigations of proteins," Adv. Colloid Interface Sci. **105**(1-3), 201–328 (2003).

1. Introduction

Measurements of cholesterol amounts have long been used in medical examinations. Recently, the importance of cholesterol's qualitative aspects has been pointed out along with its quantitative features. Cholesterol in human blood plasma is categorized into some groups: chylomicron (CM), very low density lipoprotein (VLDL), intermediate density lipoprotein (IDL), low-density lipoprotein (LDL), and high-density lipoprotein (HDL). The amounts of LDL and HDL have been used as representative parameters to indicate the physiological conditions of subjects, such as a metabolic syndrome. The LDL can be categorized further into two groups: large, more buoyant LDL (lLDL) and small, dense LDL (sdLDL). They differ not only in their size and density but also in their physicochemical composition. The strong correlation between the amount of the sdLDL and coronary diseases is widely acknowledged. Therefore, the quantitative evaluation of the fraction of sdLDL in total LDL has become clinically important [1–4].

Different laboratory techniques to quantify lipoprotein amounts have been proposed, such as high performance gel-filtration chromatography [1], ultracentrifugation [2, 5], nuclear magnetic resonance (NMR) [5], electrophoresis [5–8], and precipitation methods [9]. However, these methods are complicated and time-consuming.

To answer the above demand and to overcome problems of present techniques, we have applied a method of dynamic light scattering (DLS). Using this method, we can obtain the size information of scatterers by measuring the temporal autocorrelation of intensity fluctuation of scattered light. This technique requires no long measurement time in principle. It can be conducted using a compact device, which makes point-of-care testing (POCT) possible.

Using the DLS technique, we can estimate the size distribution of the scattering particles in the size range of LDL or 20–30 nm. The estimated size distribution is accurate when the size distribution is monomodal: when it has a distinct single peak. Some attempts to evaluate the fraction of a scattering component have been made using the height (ordinate value) or the

#120694 - $15.00 USD Received 30 Nov 2009; revised 12 Feb 2010; accepted 22 Feb 2010; published 12 Mar 2010

area (integral of ordinate value) of the particle size distribution obtained in the DLS measurement [10–15]. However, the estimated size distribution's shape is known to be neither stable nor repeatable when the true distribution is bimodal or multimodal [14–17]. Moreover, previous reports show that we can separate the size distribution of each component only when the size ratio of the two components is greater than two, and when the amount of smaller scatterers is greater than that of larger scatterers [16, 17]. The size ranges of sdLDL and lLDL are typically 20–25 nm and 23–30 nm, and the amount of sdLDL is not necessarily much larger than that of lLDL. Rasteiro et al. showed that the conventional inversion techniques present many difficulties in estimating the fraction [17]. Therefore, it is unsuitable to estimate the sdLDL fraction from the size distribution obtained using common techniques of DLS measurement.

We have developed a new technique to estimate the sdLDL fraction directly from the measured autocorrelation function without estimation of the unstable size distribution. Here, we report the theoretical derivation of the solutions for fraction estimation of sdLDL using the autocorrelation function obtained from DLS measurements. The effect of undesired large particles on the autocorrelation function can be eliminated by pre-processing of the autocorrelation function. The applicability and effectiveness of the proposed techniques are examined using experiments with latex standard particles and LDL of human serum.

2. Theoretical derivation of the weight fraction

2.1 Dynamic light scattering

Temporal autocorrelation function $g^{(1)}(\tau)$ of scattered electric field $E(t)$ is given as [18]

$$g^{(1)}(\tau) = \langle E(t)E(t+\tau)\rangle = \exp(-\Gamma\tau), \tag{1}$$

where τ is the correlation time. The decay constant Γ is given as $\Gamma = q^2D$, where D is the translational diffusion coefficient and q is the magnitude of the scattering vector given as $q = (4\pi n/\lambda)\sin(\theta/2)$, where n, λ, and θ respectively signify the refractive index of the medium, the wavelength of light, and the scattering angle.

For a diluted solution of non-interacting spheres, with a single size, or a monodisperse case, the hydrodynamic diameter d_h of the sphere is obtained from the Stokes–Einstein equation as

$$d_h = \frac{kT}{3\pi\eta D} = \frac{kTq^2}{3\pi\eta\Gamma}, \tag{2}$$

where k, T, and η are, respectively, the Boltzmann's constant, the absolute temperature and the viscosity of the medium.

In DLS, we measure the correlation function $g^{(2)}(\tau)$ of the scattered intensity $I(t)$ instead of $g^{(1)}(\tau)$, where

$$g^{(2)}(\tau) = \langle I(t)I(t+\tau)\rangle. \tag{3}$$

Furthermore, $g^{(1)}(\tau)$ is obtained from the measured $g^{(2)}(\tau)$ using the Siegert relation as

$$g^{(1)}(\tau) = \sqrt{g^{(2)}(\tau) - 1}. \tag{4}$$

Therefore, in a monodisperse case, we can obtain the size of the scatterer using Eqs. (3), (4) and Eqs. (1), (2).

In a polydisperse case, $g^{(1)}(\tau)$ is given as the weighted mean of the size distribution function as [16,19],

$$g^{(1)}(\tau) = \frac{\int_0^\infty i(r)\,g^{(1)}(\tau,r)\,dr}{\int_0^\infty i(r)\,dr} = \frac{\int_0^\infty i(r)\exp(-\alpha\tau/r)\,dr}{\int_0^\infty i(r)\,dr}, \tag{5}$$

#120694 - $15.00 USD Received 30 Nov 2009; revised 12 Feb 2010; accepted 22 Feb 2010; published 12 Mar 2010

where $\alpha=q^2kT/6\pi\eta$ and r represents the size of the scatterer, i.e. a radius of a spherical particle. Furthermore, $i(r)$ signifies the intensity size distribution or the amplitude distribution of scattered light intensity with respect to size r. In the measurement of DLS, the size distribution $i(r)$ is obtainable using conventional data processing algorithms such as CONTIN and NNLS [20]. When an accurate $i(r)$ is available, it is not difficult to obtain the fraction of specific scatterers in a known size range. However, the size distribution obtained with these techniques is often unstable and non-repeatable, particularly in the polydisperse case, as described above. Therefore, we have attempted to develop a different technique to obtain the fraction of one kind of scatterers in a bimodal size distribution.

2.2 Fraction estimation methods

We consider the case of a bimodal size distribution, i.e. the case in which the scatterers consist of those with two size ranges.

2.2.1 Fraction for narrow size distributions

When the size distributions shows two distinct modes of sizes, we assume it to be a linear sum of the Dirac's delta functions, or

$$i(r) = I_s\delta(r-r_s) + I_l\delta(r-r_l), \tag{6}$$

where r_s and r_l denote the typical sizes of small and large components of scatterers. Subscripts s and l hereinafter represent the small and the large components of scatterers. The intensity weights I_s and I_l are given as $I_s = \int_0^\infty i_s(r)dr \approx \int_a^b i(r)dr$, $I_l = \int_0^\infty i_l(r)dr \approx \int_c^d i(r)dr$, where [a, b] and [c, d] respectively stand for the size ranges of small and large scatterers. It is evident that $a \le r_s \le b$ and $c \le r_l \le d$. Then, using Eq. (5) the autocorrelation function of the electric field scattered from the mixed scatterers is given as [13, 16]

$$g_{sl}^{(1)}(\tau) = \frac{\int_0^\infty i(r)e^{-\frac{\alpha}{r}\tau}dr}{\int_0^\infty i(r)dr} = \frac{I_s e^{-\frac{\alpha}{r_s}\tau} + I_l e^{-\frac{\alpha}{r_l}\tau}}{I_s + I_l}. \tag{7}$$

If we define the intensity fraction of the small particles as $X_I = I_s/(I_s+I_l)$, then Eq. (7) reduces to

$$g_{sl}^{(1)}(\tau) = X_I e^{-\frac{\alpha}{r_s}\tau} + (1-X_I)e^{-\frac{\alpha}{r_l}\tau}, \tag{8}$$

and the fraction is obtainable as

$$X_I = \frac{g_{sl}^{(1)}(\tau) - e^{-\frac{\alpha}{r_l}\tau}}{e^{-\frac{\alpha}{r_s}\tau} - e^{-\frac{\alpha}{r_l}\tau}}. \tag{9}$$

In this way, we can estimate the fraction using the measured autocorrelation function $g_{sl}^{(1)}(\tau)$ and the typical sizes of the two scatterer components: r_s and r_l.

If the sizes r_s and r_l are sufficiently close ($(r_l - r_s)/(r_l + r_s) << 1$) such as in the LDL case, the autocorrelation function can be approximated as $g_{sl}^{(1)}(\tau) \approx \exp(-\alpha\tau/r_{sl})$, where r_{sl} is the typical size of the two-component scatterers, or $r_s \le r_{sl} \le r_l$. In the case of LDL, $\alpha\tau/r_s - \alpha\tau/r_l < 1$ and $\alpha\tau/r_{sl} - \alpha\tau/r_l < 1$ for most of the correlation time τ. Then Eq. (9) can be approximated in a much simpler form as

#120694 - $15.00 USD Received 30 Nov 2009; revised 12 Feb 2010; accepted 22 Feb 2010; published 12 Mar 2010

$$X_I \approx \frac{\frac{1}{r_{sl}} - \frac{1}{r_l}}{\frac{1}{r_s} - \frac{1}{r_l}}. \tag{10}$$

In clinical applications, the weight fraction is more commonly used rather than the fraction of scattered intensity. We define the weight fraction of small particles as $X_W = W_s/(W_s+W_l)$, $W_s = \int_0^\infty w_s(r)dr$, $W_l = \int_0^\infty w_l(r)dr$, where W and $w(r)$ respectively represent the mass-weight and the size distribution of weight. The LDL particles are much smaller than the wavelength of light. Therefore, the scattered light shows the characteristics of the Rayleigh scattering. The scattered intensity of the Rayleigh scattering is proportional to the square of the particle's volume [20]. Consequently, for a narrow size distribution, X_W can be estimated from X_I as

$$X_W = \frac{X_I r_l^3}{X_I(r_l^3 - r_s^3) + r_s^3}. \tag{11}$$

In the DLS measurement, the typical size can be evaluated as the mean size of size distribution using common algorithms such as the cumulant method [21, 22]. Therefore, we first evaluate typical sizes r_s and r_l as the mean sizes m_s and m_l in the DLS measurement using pure samples of small and large scatterers. Then, the weight fraction can be estimated as

$$X_W = \frac{X_I m_l^3}{X_I(m_l^3 - m_s^3) + m_s^3}, \tag{12}$$

where $X_I = \left(1/m_{sl} - 1/m_l\right)/\left(1/m_s - 1/m_l\right)$ and m_{sl} is the mean size evaluated in the DLS measurement with the sample solution of interest.

2.2.2 Fraction for rectangular size distribution

The assumption of a narrow distribution described above is applicable to special cases such as artificially manufactured particles. In the case of LDL, however, the size distribution is too wide to be approximated as the Dirac's delta function. Instead of the typical sizes, size ranges are often available. Therefore, we derived the solution for the weight fraction of small scatterers in the case of rectangular size distributions.

We assume the size distribution of weight as

$$w(r) = W_s\left[u(r-a) - u(r-b)\right] + W_l\left[u(r-c) - u(r-d)\right], \tag{13}$$

where $u(r)$ is a unit step function, and where $[a, b]$ and $[c, d]$ respectively denote the size ranges of small and large scatterers. In most cases, b is smaller than or equal to c, but the following formulae are also valid in the case of $b > c$.

As described above, the scattered intensity is proportional to the square of the particle's volume in the Rayleigh scattering. Therefore, the autocorrelation function can be written as

$$g^{(1)}(\tau) = \frac{\int_0^\infty i(r)\,g^{(1)}(\tau,r)dr}{\int_0^\infty i(r)dr} = \frac{\int_0^\infty w(r)r^3 g^{(1)}(\tau,r)dr}{\int_0^\infty w(r)r^3 dr} = \frac{\int_0^\infty n(r)r^6 g^{(1)}(\tau,r)dr}{\int_0^\infty n(r)r^6 dr}, \tag{14}$$

where $i(r)$, $w(r)$, and $n(r)$ respectively signify size distributions of scattered intensity, scatterers' weight and scatterers' number.

Substituting Eq. (13) to the middle part of Eq. (14), we obtain the autocorrelation function for bimodal size distribution of weight as

#120694 - $15.00 USD Received 30 Nov 2009; revised 12 Feb 2010; accepted 22 Feb 2010; published 12 Mar 2010

$$g_{sl}^{(1)}(\tau)=\frac{W_s\int_a^b r^3 e^{-\frac{\alpha\tau}{r}}\,dr+W_l\int_c^d r^3 e^{-\frac{\alpha\tau}{r}}\,dr}{W_s\int_a^b r^3\,dr+W_l\int_c^d r^3\,dr}. \tag{15}$$

We can calculate the definite integral as

$$\int_a^b r^3 e^{-\frac{\alpha\tau}{r}}\,dr=f(b)-f(a), \tag{16}$$

where

$$f(r)=e^{-\frac{\alpha\tau}{r}}\left(\frac{r^4}{4}-\frac{\alpha\tau r^3}{12}+\frac{\alpha^2\tau^2 r^2}{24}-\frac{\alpha^3\tau^3 r}{24}\right)+\frac{\alpha^4\tau^4}{24}\Gamma(0,\frac{\alpha\tau}{r}). \tag{17}$$

In that equation, Γ(0, z) is the incomplete gamma function for z > 0, or

$$\Gamma(0,z)=\int_z^\infty \frac{e^{-x}}{x}dx=\cfrac{e^{-z}}{z+1-\cfrac{1}{z+3-\cfrac{4}{z+5-\cfrac{9}{z+7-\ldots}}}}. \tag{18}$$

Therefore Eq. (15) becomes

$$g_{sl}^{(1)}(\tau)=\frac{W_s\left[f(b)-f(a)\right]+W_l\left[f(d)-f(c)\right]}{\frac{W_s(b^4-a^4)}{4}+\frac{W_l(d^4-c^4)}{4}}. \tag{19}$$

For the bimodal size distribution given in Eq. (13), the weight fraction of small scatterers is given as

$$X_W=\frac{W_s(b-a)}{W_s(b-a)+W_l(d-c)}. \tag{20}$$

Using Eqs. (19) and (20), we can obtain the weight fraction as a function of the autocorrelation function as

$$X_W=\frac{\{4[f(d)-f(c)]-(d^4-c^4)g_{sl}^{(1)}(\tau)\}(b-a)}{\{4[f(d)-f(c)]-(d^4-c^4)g_{sl}^{(1)}(\tau)\}(b-a)-\{4[f(b)-f(a)]-(b^4-a^4)g_{sl}^{(1)}(\tau)\}(d-c)}, \tag{21}$$

where *f*(*r*) is given as Eq. (17).

3. Method of experiment

3.1 Polystyrene latex beads

To test the effectiveness of the proposed techniques in practice, the controlled solutions of latex particles (polystyrene spheres) have been prepared. Standard latex particles of two kinds (21±5.7 nm and 28±6.1 nm dia.; Magspheres Inc.) were used. The 10% latex solutions of both sizes were diluted with pure water to 0.1%. Then 11 samples were prepared by mixing these two solutions in different weight fractions: 0, 0.1, 0.2, 0.3, 0.4, 0.5, 0.6, 0.7, 0.8, 0.9, and 1. Fractions 0 and 1 correspond respectively to the samples that contain only large particles and small particles.

3.2 Lipoprotein

Large LDL (relative density, *d* = 1.019–1.044 kg/L) and sdLDL (*d* = 1.044–1.063 kg/L) were separated from human serum by sequential ultracentrifugation (Optima™ Max

#120694 - $15.00 USD Received 30 Nov 2009; revised 12 Feb 2010; accepted 22 Feb 2010; published 12 Mar 2010

ultracentrifuge; Beckman Coulter Inc.) with a near vertical tube rotor (MLN-80; Beckman Coulter Inc.). Serum (2 ml) was mixed with 6 ml KBr solution (d = 1.023 kg/L); the mixture was centrifuged at 40,000 rpm for 20 h at 15°C. The 2.5 ml supernatant containing lipoproteins (d < 1.019 kg/L) was removed and 2.5 ml KBr solution (d = 1.099 kg/L) was added to the infranatant. After centrifugation at 50,000 rpm for 18 h at 15°C, 2.5 ml supernatant (d < 1.044 kg/L) containing large LDL was obtained. Then, 2.5 ml of the KBr solution (d =1.105 kg/L) was added to the infranatant. It was centrifuged at 50,000 rpm for 18 h at 15°C. Finally, 2.5 ml supernatant (d < 1.063 kg/L) containing sdLDL was obtained, and the infranatant was used as the sample solution that contains HDL and the smaller proteins with higher density. The accuracy of these processes was confirmed using polyacrylamide gel electrophoresis (LipoPhor; Quantimetrix Corp.) as the purity of each separated fraction. Furthermore, serum lipids were measured using automated enzymatic method with a commercial kit (Denka Seiken Co., Ltd., Tokyo, Japan): T-CHO(S) for total cholesterol (TC). After this separation process, both sdLDL and large LDL were diluted with sterile 0.9% saline solution to make their concentrations equal. Then, they were mixed to prepare the LDL samples in different weight fractions.

3.3 Dynamic light scattering system

The autocorrelation function of scattered intensity $g^{(2)}(\tau)$ was measured using a DLS system (FDLS-3000; Otsuka Electronics Co., Ltd.). The laser power was 100 mW and the wavelength was 532 nm. The scattered light was detected at θ= 90°. The DLS system temperatures were respectively set to 25°C and at 37°C for the latex particles and the LDL experiments. The sample solution was contained in a 178 mm × 5 mmϕ glass tube (Optima USA, Inc.). A water bath was used to keep the temperature of the samples constant. Measurement of the scattered intensity fluctuation was repeated 100 times with each sample.

4. Elimination of large scatterer effect

In practical measurements of DLS, the existence of undesired scatterers and aggregates often causes error in the size estimation of scatterers. From Eq. (5), we can express the effect of the undesired scatterers as

$$g_m^{(1)}(\tau) = \frac{I_S g_S^{(1)}(\tau) + I_N g_N^{(1)}(\tau)}{I_S + I_N}, \tag{22}$$

where $g_m^{(1)}(\tau)$ is the measured autocorrelation function, and S and N respectively denote the signal and the noise components. In practice, $g_m^{(1)}(\tau)$ is obtained from the measured intensity autocorrelation function $g_m^{(2)}(\tau)$ using Eq. (4).

As described previously, the scattered intensity of the Rayleigh scattering is proportional to the sixth power of the particle size. Consequently, the major part of the noise component of Eq. (22) comes from larger particles than LDL. This size difference makes clear distinction between the autocorrelation functions of the signal and noise components. Figure 1 shows that a typical measured autocorrelation function $g^{(1)}(\tau)$ is divisible into two parts. According to a report of an earlier study [17], the correlation function is divisible into different time periods; the latter is dominated by noise. Therefore, we can separate $g_S^{(1)}(\tau)$ from $g_N^{(1)}(\tau)$ using the curve fitting technique with two exponential components. In the following experiments, the $g_{sl}^{(1)}(\tau)$ in the previous chapter was extracted as the $g_S^{(1)}(\tau)$ in Eq. (22) from the measured autocorrelation function $g_m^{(1)}(\tau)$ using the curve fitting technique with Eq. (22). The curve was fitted using nonlinear least squares fitting [23].

Figure 1 presents an example of this process with 28 nm latex spheres. The solid line shows the measured autocorrelation function $g_m^{(1)}(\tau)$ of a monodisperse solution of 28 nm latex spheres in the DLS measurement. Deviation from the theoretical straight line is evident. This figure shows that the curve fitting with two exponential components yielded satisfactory agreement. By subtracting the component of large scatterers according to Eq. (22), we were

#120694 - $15.00 USD Received 30 Nov 2009; revised 12 Feb 2010; accepted 22 Feb 2010; published 12 Mar 2010

able to extract the major component (thick dotted line) for the desired autocorrelation function $g_{sl}^{(1)}(\tau)$.

The effectiveness of this data-processing was examined using experiments with monodisperse solutions of different kinds. The mean sizes were estimated using the cumulant method in the DLS measurement. Table 1 presents the results. With the elimination process, for latex particles, the results agreed well with those provided by the manufacturer. Without the elimination process, the mean sizes were overestimated, which suggests that the larger size often estimated with DLS can be attributed to the existence of large particles such as aggregates. In the LDL particle cases, the mean sizes were 21.7 nm and 23.6 nm for sdLDL and lLDL, respectively, which agreed well with those reported in the literature [24, 25]. These results suggest the effectiveness of the data processing technique proposed here.

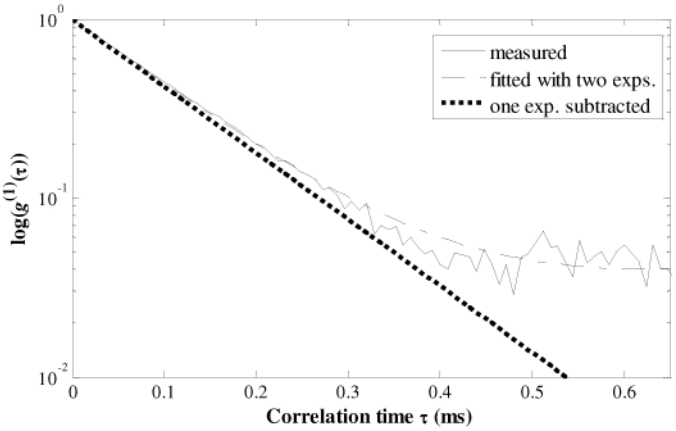

Fig. 1. Elimination of large particles effect from measured normalized autocorrelation function $g_m^{(1)}(\tau)$ by subtracting one exponential component in two-exponential fitting.

Table 1. Mean sizes estimated in DLS with the elimination process of large scatterer effect

Sample	Without elimination	With elimination
latex 21 nm	24.7 nm	21.2 nm
latex 28 nm	31.4 nm	28.8 nm
sdLDL	36.9 nm	21.7 nm
lLDL	28.1 nm	23.6 nm

5. Experimental verification

5.1 Fraction estimation with standard particles

The feasibility of the proposed fraction estimation techniques was examined using standard latex particles with known size distributions. The measurements were repeated six times for each sample with different fractions. The autocorrelation function $g_m^{(1)}(\tau)$ was obtained from the measured intensity autocorrelation function $g_m^{(2)}(\tau)$ in DLS measurement according to the Siegert relation in Eq. (4). Then $g_{sl}^{(1)}(\tau)$ was obtained from the $g_m^{(1)}(\tau)$ by the elimination process using Eq. (22).

In the first proposed technique, namely Method#1, the mean size m_{sl} of the testing solution was estimated from the $g_{sl}^{(1)}(\tau)$ using the common cumulant method. The weight fraction X_W was estimated using Eq. (12) using this m_{sl} and the known mean sizes m_s and m_l.

#120694 - $15.00 USD Received 30 Nov 2009; revised 12 Feb 2010; accepted 22 Feb 2010; published 12 Mar 2010

In the second proposed technique, or Method#2, we estimate the weight fraction using Eq. (21). In this process, we respectively need the size ranges $[a, b]$ and $[c, d]$ for small and large scatterers. We assumed the size ranges using the standard deviation of the size distribution. That is $a = m_s - \sigma_s$, $b = m_s + \sigma_s$, $c = m_l - \sigma_l$, $d = m_l + \sigma_l$, where m and σ respectively represent the mean and the standard deviation of the particle size distribution. The values of m and σ were provided by the manufacturer. The weight fraction X_W was estimated from the $g_{sl}^{(1)}(\tau)$ using Eq. (21).

For comparison, the fraction was obtained using a conventional method. In the conventional method, the size distribution of the mixed solution is estimated first. Then the fraction is calculable from the estimated size distribution. To estimate the size distribution, the common CONTIN algorithm [21, 26] was applied to the same DLS data as used in the estimation above. Figure 2 presents the size distribution $f_{est}(r)$ estimated using the CONTIN algorithm. Using the curve fitting technique [23], this distribution $f_{est}(r)$ is resolved into the sum of the two Gaussian distributions, or

$$f_{est}(r) = I_s \frac{1}{\sqrt{2\pi\sigma_s^2}} \exp\left[-\left(\frac{(r-m_s)^2}{2\sigma_s^2}\right)\right] + I_l \frac{1}{\sqrt{2\pi\sigma_l^2}} \exp\left[-\left(\frac{(r-m_l)^2}{2\sigma_l^2}\right)\right], \quad (23)$$

where m_s, m_l and σ_s, σ_l respectively signify means and standard deviations of the normal distribution. An example of curve fitting with two normal distributions of fixed means and standard deviations is presented in Fig. 2.

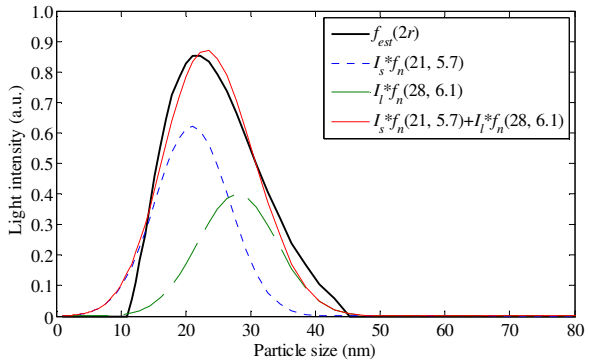

Fig. 2. Example of curve fitting with two normal distributions: $f_{est}(2r)$, size distribution estimated by DLS; $f_n(m, \sigma)$, normal distribution with mean m and standard deviation σ; I_s, I_l, respective intensity weights for small and large components.

Figure 3 shows a comparison between the conventional and the proposed methods. The weight fraction of the proposed method was estimated using Eq. (21), or Method#2. The means of estimated fractions are shown in the closed circles in Fig. 3. The thick solid line is the linear regression line between the given and the estimated fractions. In the conventional method, the magnitude of each normal distribution I_s and I_l was estimated with the parameters $2m_s$ = 21 nm, $2m_l$ = 28 nm, $2\sigma_s$ = 5.7 nm, and $2\sigma_l$ = 6.1 nm. The intensity fraction X_I was estimated as $X_I = I_s/(I_s+I_l)$, and the weight fraction X_W was obtained with Eq. (12), which is shown in the open circles in Fig. 3. More estimation processes were involved in this indirect estimation. Therefore, the agreement between the given and the estimated fraction was poor.

Figure 4 portrays a comparison between the proposed methods, or Method#1 and Method#2. They have different features. Method#1 is based on the theoretical model with very narrow size distribution for each component. It requires only the typical sizes of the two components beforehand. The fraction can be estimated from the mean size of the mixed sample. Method#2 is applicable to cases with a wider size distribution. It requires the size ranges of the two components beforehand, and the fraction can be estimated from the

#120694 - $15.00 USD Received 30 Nov 2009; revised 12 Feb 2010; accepted 22 Feb 2010; published 12 Mar 2010

autocorrelation function of the mixed sample measured in DLS. Results of the fraction estimation obtained using these methods are presented in Fig. 4.

The estimated fraction sometimes becomes negative attributable to the noise and the artifacts in the measurement. Therefore, the following corrections were made. If $m_{sl} < m_s$, then $m_{sl} = m_s$ and if $m_{sl} > m_l$, then $m_{sl} = m_l$ in the Method#1. If $X_w < 0$, then $X_w = 0$, and if $X_w > 1$, then $X_w = 1$ in Method#2. Except for a few corrected points, both results show good agreement. As expected, the result by Method#2 was much closer than that by Method#1 to the correct value shown in the broken line in Fig. 4. This is the size distributions of 21 nm and 28 nm particles were too wide to be approximated as the Dirac's delta function, and the assumption for Method#2 holds well.

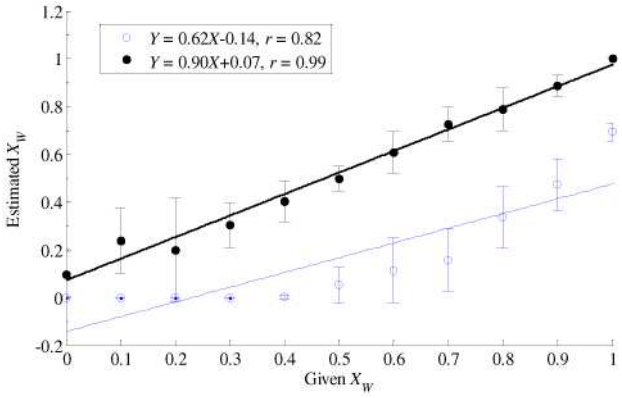

Fig. 3. Estimated results of 21 nm particles fraction in 21 nm and 28 nm mixed solution using size distribution estimation (○) and using the proposed technique (●), $n = 6$.

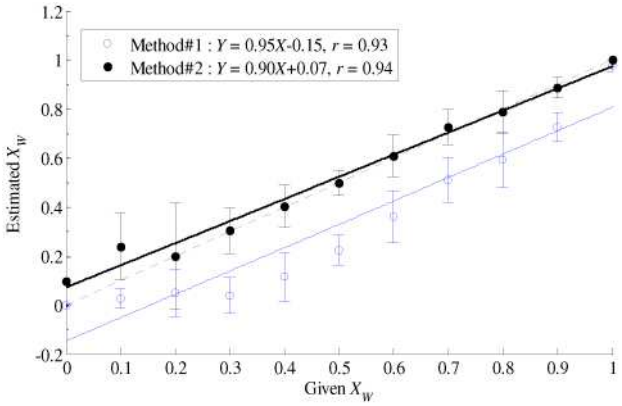

Fig. 4. Comparison between two proposed methods for 21 nm particles fraction in 21 nm and 28 nm mixed solution: Method#1 (○) and Method#2 (●), $n = 6$.

5.2 Fraction estimation of sdLDL

Finally, the proposed techniques were applied to the LDL solution to examine their effectiveness. Means for Method#1 and size ranges for Method#2 are required. The DLS measurement was made with the separated solutions of sdLDL and lLDL before making the mixed solution. The means were estimated using the common cumulant method, which is known to give an accurate mean for monomodal solution [21]. The estimated values were similar to the reported values measured in both DLS and gel gradient electrophoresis [24]. Considering these values, we respectively set the means and the ranges for sdLDL and lLDL as 21.5±2.75 nm and 23.5±2.25 nm.

#120694 - $15.00 USD Received 30 Nov 2009; revised 12 Feb 2010; accepted 22 Feb 2010; published 12 Mar 2010

Figure 5 shows the estimated weight fraction of sdLDL in total LDL using both methods. The estimation was repeated eight times. The variation of the estimated fraction was larger than in the case of standard particles. However, the correlation between the given and the estimated fractions was satisfactory. The large variation might be attributable to the mean size difference between the two components, which was apparently smaller in the LDL case ($(r_l-r_s)/(r_l+r_s)$ ≈0.1) than in the standard particle case ($(r_l-r_s)/(r_l+r_s)$ ≈0.35). This made the autocorrelation functions for each component more similar in the LDL case. The estimated result was more vulnerable to noise and artifacts in the measurement of the autocorrelation function than in the standard particle case.

The estimated fractions were smaller than the given fractions in both cases of Methods #1 and #2, apparently because of the greater number of particles larger than sdLDL. The fractions presented in Fig. 5 were obtained by application of the technique to suppress the effect of aggregate based on Eq. (22). Techniques that are more powerful might be needed to eliminate this effect. In practice, however, one can estimate a correct fraction using this regression line as a calibration curve as long as it is consistent throughout the measurement conditions. Comparison of results obtained using Methods #1 and #2 shows that the proposed method, based on a more realistic assumption, gives a better estimation for the fraction estimation of sdLDL.

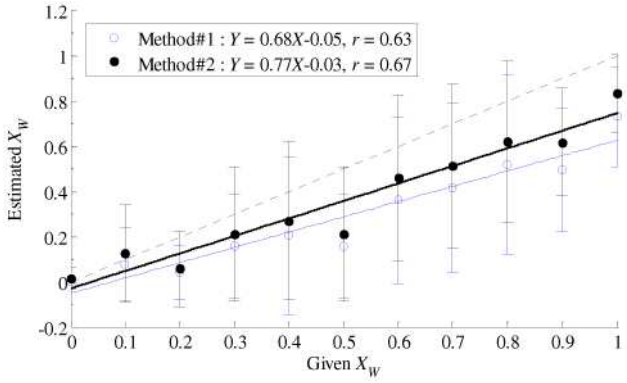

Fig. 5. Estimation of sdLDL fraction in total LDL using Method#1 (○) and using Method#2 (●), $n = 8$.

6. Conclusion

We proposed an optical measurement technique to estimate the fraction of one component of scatterers with a bimodal size distribution. It was applied to estimation of sdLDL fraction in the total LDL to make point-of-care testing for sdLDL possible. This technique is based on the dynamic light scattering measurement. Two methods were newly proposed to obtain the fraction based on different assumptions. In one method, the fraction of one component in the scatterers with bimodal size distribution is estimated from the total mean size in the DLS measurement. For this method, the mean sizes for each of the two components of scatterers are required. In another method, the fraction is estimated from the autocorrelation function of the scattered intensity fluctuation. For this method, the size ranges for each of the two components are required. An appropriate mean size and autocorrelation function were obtained by eliminating the effect of large scatterers in the DLS measurement. The feasibility of the proposed techniques was verified using experiments with latex standard particles and LDL samples with known fractions. With these proposed methods, we can estimate the sdLDL fraction with a simpler and shorter procedure than those of conventional techniques. They will provide new possibilities to realize point-of-care testing of sdLDL.

#120694 - $15.00 USD Received 30 Nov 2009; revised 12 Feb 2010; accepted 22 Feb 2010; published 12 Mar 2010

Acknowledgements

The authors thank Professor Masahiro Tsuji of Health Sciences University of Hokkaido Hospital for his valuable advice related to this research. A part of this research was supported by a Grant-in Aid for Scientific Research from the Japan Society for the Promotion of Science.

#120694 - $15.00 USD Received 30 Nov 2009; revised 12 Feb 2010; accepted 22 Feb 2010; published 12 Mar 2010